Plant Archives Vol. 21, Supplement 1, 2021 pp. 456-463 e-ISSN:2581-6063 (online), ISSN:0972-5210

Plant Archives

Journal homepage: http://www.plantarchives.org
doi link : https://doi.org/10.51470/PLANTARCHIVES.2021.v21.S1.070

EFFICACY OF ACELLULAR-LYOPHILIZED HUMAN UMBILICAL CORD ECM-POWDER GUIDED BY BOVINE URINARY BLADDER MATRIX CONDUIT FOR PERIPHERAL NERVE REPAIR IN DOGS MODEL

Ali A. N. AL-Zaidi[1*], Hameed A.K.Al-Timmemi[2] and Zeyad A. Shabeeb[3]

[1]Department of Clinics Sciences, College of Veterinary Medicine, University of Kufa, Iraq
[2]Departments of Surgery and Obstetrics, College of Veterinary Medicine, University of Baghdad, Iraq
[3]The National Center of Hematology, Al-MustansiriyahUniversity, Iraq
*Corresponding authorE-mail: alizent95@yahoo.com

ABSTRACT

Peripheral nerve possesses the inherent ability to regrow and recover the following injury. However, nerve regeneration is often slow and incomplete due to limitations associated with the local microenvironment during the repair process. Manipulation of the local microenvironment at the site of nerve repair, therefore, represents a significant opportunity for improvement in downstream outcomes. Sixteen (16) local breed dogs were divided equally into acellular bovine urinary bladder matrix conduit as conduit group (CG) and acellular bovine urinary matrix conduit filled with acellular and lyophilized human umbilical cord ECM scaffolds as scaffold group (SG). This study aimed to investigate the efficacy of acellular and lyophilized human umbilical cord ECM scaffold as an intraluminal filler of acellular bovine urinary matrix conduit onthe regeneration of 1cm radial nerve defect in dog's model as histopathological analysis. Histopathological examinations of the proximal nerve stump in the (CG) showed mild adherence surrounding acoaptated area, few vacuolations, and profuse of collagen at the peri and epineurium. The coaptatedsite showed the degeneration, disorientationof nerve fibers, and invasion of inflammatory cells with a high number of macrophages and lymphocytes, whileintraneural scar tissues were seen in the distal segment at the 112th post-operation day (POD). The histopathological sections of (SG) showed the activated Schwann cells, good myelination, minimum scar tissue, good orientation, and remarkable angiogenesis at the 112th POD.Theacellular and lyophilized human umbilical cord ECM scaffold is capable of promoting the regeneration of radial nerve defects.

Keywords: Gap nerve injury, nerve graft, regeneration, radial nerve, UBM& HUC-Scaffolds

Introduction

Peripheral nerve defects always result in functional loss and remain an intractable challenge for clinical researchers (Sabongi *et al*., 2015). Remarkably, the peripheral nervous system (PNS) is capable to regenerate after minor injuries such as segmental demyelination (neurapraxia) or the disruption of axons when most of the surrounding connective tissue remains intact (axonotmesis). Severe injuries include nerve transection (neurotmesis) or the loss of nervous tissue that exceeds the PNS' inherent regenerative ability. Such conditions commonly entail scar tissue infiltration and/or neuroma formation causing pain and permanent deficits that severely affect the patient's life (Hokeand Brushart, 2010). Despite advances in microsurgical technique and extensive studies on nerve repair, the surgical re-innervation methods produce only moderate results and full functional recovery after nerve injury is seldom achieved (Chen *et al*., 2011). Therefore, methods that accelerate or improve re-innervation following reconstruction of peripheral nerve are of significant clinical interest. One opportunity for functional improvement after nerve reconstruction or grafting is manipulation of the microenvironment at the site of nerve repair to promote modulation of the host inflammatory response and to promote Schwann cell migration and axon extension across the repair site (Khuong *et al.,* 2014. Lavasani *et al.,* 2014; Cattin *et al.,* 2015). Extended axonal regrowth cannot occur without closely apposed Schwann cells (SC) and the specificity of this process is enhanced both by extracellular matrix (ECM) components, such as collagen IV or laminin, which provide basement membrane support for SC migration and by neovascularization promoted by certain macrophage subsets (Cattin *et al.,* 2015). Nerve autografts contain an intact nervous architecture, Schwann cell support, and extracellular matrix (ECM) molecules that offer the best conditions possible for nerve recovery (Houshyar *et al.,* 2019). Nevertheless, the availability of donor nerves is limited and donor nerve innervated tissue suffers from functional loss. The second incision site bears the additional risk of donor site morbidity, neuroma formation, and pain (Faroni *et al.,* 2015; Siemers and Houschyar, 2017). Many groups have proposed different approaches focus on the improvement of artificial nerve

conduits enriched with biological components such as growth factors, peptides, or ECM molecules (Gonzalez-Perez *et al.,* 2017; Yao *et al.,* 2018). Although artificial nerve conduits can only provide mechanical support to the nerve as there is no extracellular matrix component in the lumen to promote the cavity support structure for axon growth (Chen and Shen, 2017; Liu *et al.,* 2017). Animal-based studies (di Summa *et al.,* 2011; Jesuraj *et al.,* 2014; Hoben *et al.,* 2015) have shown positive outcomes using decellularized conduits to repair peripheral nerve injuries. The decellularized extracellular matrix has a three-dimensional network structure, which retains proteins and carbohydrates, giving structural support to the nerve. This promotes cell migration, proliferation, differentiation and regulation of intercellular communication (Gonzalez-Perez *et al.,* 2013). On the other hand biomimetic nerve guidance conduits with biomaterial-based intra-luminal scaffolds have been developed. These internal lumen scaffolds are designed to resemble the endoneurial structure of peripheral nerve, further create a desirable microenvironment and act as contact topographical cues to enhance axonal regeneration (Badylak *et al.,* 2009; Kanno *et al.,* 2015), in all four major tissue types, including connective (Brown *et al.,* 2011), skeletal muscle (Badylak *et al.,* 2016), epithelial (Badylak *et al.,* 2016), and even nervous tissues (Meng *et al.,* 2014), with ECM derived from younger tissues often more efficacious (Li *et al.,* 2014). Mechanistically, ECM bio scaffolds and/or ECM derived factors have been shown to positively modulate the innate immune response (Dziki *et al.,* 2017), and increase site-appropriate tissue remodeling over scarring (Remlinger *et al.,* 2013), increase neovascularization, and promote Schwann cell migration and differentiation (Fercana *et al.,* 2017), neurogenesis, and neurodifferentiation (Faust *et al.,* 2017). Moreover, ECM is a highly tunable platform that can be modified mechanically and biochemically based on the nature and the scope of the injury(Hong *et al.,* 2011). Therefore the aim of the present study is to evaluate the implantation of acellular and lyophilized human umbilical cordas intraluminal ECM scaffold for peripheral nerve regeneration using decellularized urinary bladder matrix conduit as histopathological analysis in dog's model.

Materials and Methods

Experimental Design

Sixteen male adult local breed dogs aged (8-12) months and weighting (15-20)kg were divided in to two groups consisting of (8) animals each. In the first group, the radial nerve was transected of (1 cm)and the resulted gap was bridged by (14mm) acellular bovine urinary bladder matrix (UBM) conduit using (0-6) nylon perineural sutures of the proximal and distal stumps. Which served as conduit group (CG), While the second group was treated with acellular bovine urinary bladder matrix conduit which was filled with acellular human umbilical cord (HUC) tissue ECM scaffold and sutured as conduit group and served as scaffold group (SG). All animals were housed in individual cages, fed with commercial food and water. The animals were kept in their respective cages for 15 days for acclimatization before the surgical operation. Broad-spectrum antibiotic injection of ceftriaxone 22 mg/kg was given IM twice daily for five days. Antihelmintic injection of 0.2 mg/kg Ivermectin (Ivomec, Holland) 0.4 ml/kg SC was given on the first day and day 14 of acclimatization. All Procedures used in this study were approved by scientific committee, College of Veterinary Medicine, University of Baghdad-Iraq. All animals from each group were sacrificed at the 56th and 112th post operation day.

In Vitro Protocols

Fabrication of Conduit Derived from Bovine UBM-ECM

Fresh urinary bladders were collected as whole from slaughtered cows at the local abattoir and the urinary bladder matrix (UBM) was prepared as a decellularized scaffold, according to method described by Eberli *et al*. (2011).The urinary bladder was filled with tap water to facilitate the trimming and removing of external connective tissues and adipose tissue by scissors then washed with tap water. Tunica serosa, tunica muscularis and most of the muscularis mucosa were mechanically delaminated from the bladder tissue by scraping with the knife, and finally flattened rectangular sheet (Fig.1.A). The remaining (sub-mucosal layer) was then decellularized and disinfected by immersion the sheet in a mixtureof 0.1% peracetic acid (PAA) and 4% ethanol solution on a shaker for two hours. After that, the ECM was rinsed in phosphate buffered saline (PBS) (pH 7.4) to returned the pH to 7.4, containing 100 IU/ml penicillin, 100 µg/ml streptomycin and 100 µg/ml amphotericin together at 25 °C with trembling, then in two changes deionized water and finally one change of PBS, 15 min each. The resulted decellularized ECM scaffolds were terminally sterilized by immersion in 0.1% PAA solution titrated to pH 7.0 at room temperature for five hours (Rosario *et al*., 2008). (Fig.1.B). Finally the disinfected and decellularized sheets were cut at certain sizes (Fig.1C) and used for wrapping the UBM around the stainless steel pin at different sizes depending on the diameter of the tube (inner diameter of 1.68 – 0.09 mm, a wall thickness of 0.57 – 0.02 mm, and a length of I2 mm). Then, they were adhered to the two edges of the tube (Fig. 1D) by using biological adhesive made of egg albumen.

Fabrication of Powder Derived from HUC-ECM

The human umbilical cord tissue powder was obtained as described by Koc *et al.* (2017). Human umbilical cords (HUCs) were obtained from women with healthy pregnancies during caesarean deliveries at the end of gestation after signing informed consents. Umbilical cords (UCs) were collected from Al-Yarmouk Teaching Hospital, Iraqi hospitals. About 20-25 cm of umbilical cord tissue was collected in phosphate-buffered saline (PBS) (Sigma, USA) supplemented with antibiotics, 100 U/ml penicillin and 100 μg/ml streptomycin (Gibco, USA) and transported to the laboratory. UCs were washed with PBS under a sterile laminar flow cell culture hood and cut into 5 cm segments. The segments were cut longitudinally, and blood vessels were removed, and then transferred in 50 ml conical tube to frozen (24 h at -20°C), aseptically transported into the laboratory, and subsequently thawed and transversely cut into pieces (~0.5cm length). Tissue pieces were agitated in 0.1M phosphate-buffered saline bath (48h at 4 $^{\circ}$C). The PBS bath was exchanged three times before the tissue pieces were soaked in 0.02% trypsin/0.05% EDTA (120 min. with shaking) and afterward in 0.1% peracetic acid in 4.0% ethanol bath (120 min. with shaking), and then socked in a series of PBS and deionized water (dH2O) for 15 min two times of each (Fig. 2A). The decellularized HUC-ECM were allowed to set slightly before being transferred to −20°C for 24 hours then transferred to the deep freezer at -80°C for 5 days. The tissue was subsequently lyophilized for 24 hours at

-56°C under 5 mm Hg in a lyophilizer (FTS Systems Bulk Freeze Dryer Model 8–54) for lyophilization till it is completely dried. The samples were then grinded into a fine powder for 20 min. with mixer mill device. Each sample was sterilized by oven at 60°C over night; then kept in a sterile container until use (Fig. 2. B).

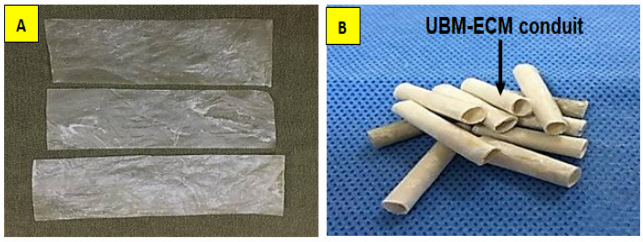

Fig. 1: Photograph showing the conduit fabrication from the bovine urinary bladder matrix. A. Disinfected and decellularized sheets were cut at certain sizes. D. Wrapping of the UBM around the stainless steel pin and fabricated conduits.

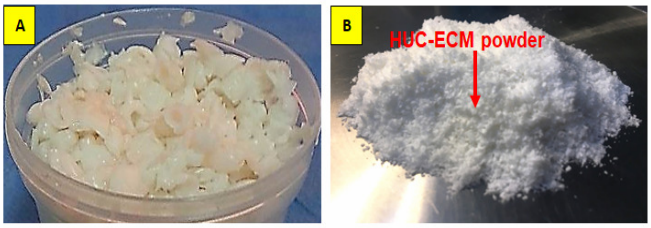

Fig. 2: Photograph showing scaffold fabrication from human umbilical cord tissue. A. HUC-ECM pieces after decellularization. B. lyophilized HUC- ECM.

Modified Surgical Procedure

The dogs were fasted for six hours before the anesthesia. Dogs were premedicated with atropine sulfate (Kepro®, Holland) in dose rate of 0.03 mg/kg, then after 10 minutes the dog was anaesthetized by a mixture of 5 mg/kg of Xylazine hydrochloride (Xyla®, Holland) and 15mg/kg Ketamine hydrochloride (Kepro®, Holland) intra-muscule respectively. Dog hair on the skin was shaved off from the lateral and medial aspect of the right front limb around the humerus up to the level of the shoulder joint and distally down to the level of the elbow joint. The skin was disinfected with chlorhexidinegluconate, Isopropyl alcohol 70% and finally with 1.8 % tincture iodine. The paw was extended by placing a latex glove over the distal extremity and securing it to the limb with a tape. The glove was covered with sterile skin towel and secured to the limb with towel clips. Then, the animal was placed on left lateral recumbency and an aperture of fenestrated drape was made on the right front limb at the targeted operation area. The proximal and central humeral diaphyses were used as landmarks through a craniolateral approach. After carefully palpation a skin incision about (5-7 cm) from the cranial border of the tubercle of the humerus and distally to the middle level of the humerus and the incision follow the normal curvature of the humerus was made. The subcutaneous fat and brachial fascia was incised along the same line; the cephalic vein was protected and isolated. The brachial fascia along the border of the brachiocephalicus muscle and lateral head of the triceps was incised bluntly to avoid rupture of the radial nerve and by aid of gelpi retractor; the lateral head of triceps brachialis and brachiocephalicus muscles were retracted to expose the nerve. Caution was used when incising the fascia along the cranial border of the triceps overlying the brachialis muscle until the radial nerve is visualized. After the radial nerve was exposed, the nerve was severed proximally by using sterile scalpel blade size (No. 10) and then distally transected the 1 cm segment mid portion of the right radial nerve. In conduit group (CG), A 14mm of acellular bovine UBM conduit was fixedat the gap and about six equidistant epineurial simple interrupted stitches were placed about 2-mm from the edges of two stumps of the transected nerve using 6-0 nylon (Monofilament, ETHICON USA) (Fig.3 A), While in the scaffold group (SG), the bovine acellular UBM conduit was filled intraluminally with (0.01mg) acellular lyophilized HUC-ECM scaffold and then sutured to the two stumps as in (CG) (Fig.3 B). Finally, the brachiocephalicus muscle and the superficial pectoral muscles were sutured to the fascia of the brachialis muscle with 3-0 Polydioxanone simple continuous sutures. Suture the subcutaneous tissue and skin with standard methods. All animals were given postoperative analgesia Tramadol hydrochloride (Trabar® Switzerland, 100 mg) 0.2 ml/kg intramuscular administered at 12-hour intervals for three consecutive days.

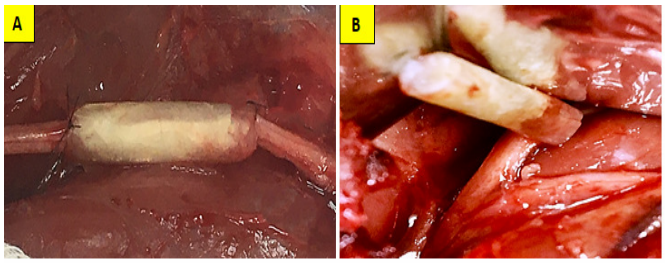

Fig. 3: Photograph showing surgical procedure. A. In the conduit group (CG), suturing of the two ends of conduit through the nerve gap using 6-0 nylon interrupted stitches. B. In the scaffold group (SG), the conduit was filled with acellular, lyophilized HUC-ECM and then sutured into the proximal and distal stumps of the nerve.

Neurohistopathological Assessment

Animals of each group were euthanized at the 56th and 112th POD using intracardial injection of pentobarbitone (Dolethal 180mg/ml) 1 ml/kg under ketamine/xylazine anesthesia. The treated right radial nerve was exposed, examined grossly and then harvested for histopathological examinations. Three specimens of 1-cm length were collected from the proximal, middle (coaptate site) and distal segments of the coaptedradial nerve. specimens were fixed in 10% neutral buffered formalin, dehydrated in a graded ethanol series, cleared in xylene, embedded in paraffin and cut into 5 µm thick sections and stained with Hematoxyline and Eosine stain All stained slides were viewed under an Olympus image analysis (BX 51 TF, with attached CC 12 camera).

Results

Neurohistopathological Findings

In the conduit group (CG), the longitudinal sections of the proximal stump of nerve showed obvious characteristics of Wallerian degeneration characterized by degeneration, vacuolation, ovoid digestive chambers, decrease in number of schwanncells, segmental demyelination and collagen deposition in the epineural region and congestion of blood vessels were also observed on day 56 PO (Fig.4 A). While the mid-portion (coaptated site) revealed invasion of inflammatory cells with a high number of macrophages and

lymphocytes, disorientation of nerve fibers, axons were thin, less compact, irregular, and discontinuous and there was adherence of the site with adjacent tissue (Fig.4 B). In the distal nerve stump, the wallerian degeneration was observed significantly as showed highly vacuolated and degenerated nerve fibers, digestive chambers and moderately irregular collagen deposits between nerve fibers, also there was low number of Schwann cells (Fig.4 C). However, the histopathological findings in the same group at the end of the 112PO, the proximal nerve stump revealed mild adhesion of the coaptated region with the adjacent tissues, the vacuolation and degeneration of the nerve fibers were fewer as compared with the previous period, there was a profuse amount of collagen fibers in the epi and perineurium, and remyelination of regenerated nerve fibers, while the aggregation of schwann cells were markedly increased in number (Fig.5 A). The histological changes at the middle stump of nerve (coaptated site) presented a few degenerated nerve fibers, increased presence of Schwann cells, improved parallel orientation of nerve fibers, deposition of fibrous tissue and inflammatory cells (Fig.5 B). The longitudinal distal nerve stump sections revealed vacuolated, degenerated nerve fibers, minimum scar tissue, improved myelination and showed inflammatory cells (Fig.5 C).The histopathological findings of the scaffold group (SG), the changes at the proximal nerve stump sections at the end of 56th POD, revealed the presence of numerous Schwann cells, new blood vessels formation, degenerated nerve fibers, vacuolation and axons infiltrated with inflammatory cells and few collagen fibers, remarkable orientated nerve fibers were also seen in this treated group (Fig.6 A). The histological findings of the middle segment (coaptated site), revealed parallel arrangement of newly formed nerve fibers with good numbers of basophilic Schwann cells, few degenerated nerve fibers, inflammatory cells and fibroblast with collagen fibers (Fig.6 B). The longitudinal section of the distal segment demonstrated Wallerian degeneration involving the ovoid and digestive chambers scattered lymphocytes with good orientation of regenerative nerve fibers (Fig.6 C). Interestingly, the sections of the proximal segment in this group at the end of 112th POD revealed the absence of degeneration and vacuolation, improvement of the parallel, packed and oriented nerve fibers, good remyelination of regenerated nerve fibers and existence of active Schwann cells (Fig.7 A). The other section of middle segment of the nerve fiber demonstrated active Schwann cells, and parallel arranged nerve fibers, as well as angiogenesis. While in the distal stump showed good orientation of the nerve fibers and remyelination, no degenerated nerve fibers, remarkable angiogenesis, and active proliferated basophilic Schwann cells (Fig.7 B). While the distal stump revealed marked good orientation of the nerve fibers and presence of plenty active basophilic Schwann cells with no degenerative nerve fibers (Fig7 C).

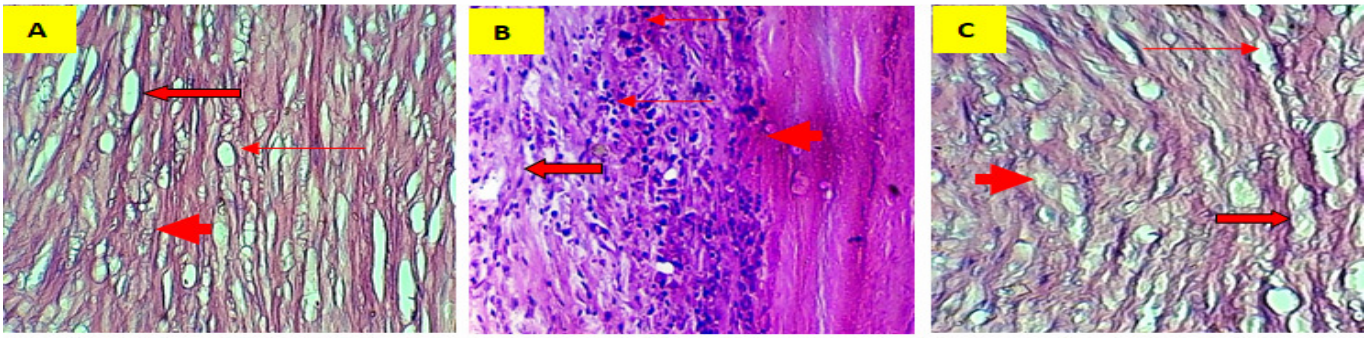

Fig. 4: Photomicrographs of the radial nerve in CG at 56th POD. A. Proximal stump shows degeneration, vacuolation (thin arrow), ovoid (thick arrow) with digestive champers of collagen (arrow head); B. Mid (coaptated site) shows aggregation of inflammatory cells (thin arrow), disoriented nerve fibers (thick arrow) with adhesion and collagen (scar tissue) (arrow head); C. Distal stump demonstrates degeneration and vacuolation (thin arrow), ovoid (thick arrow), with digestive champers of collagen (arrow head). X40 H&E.

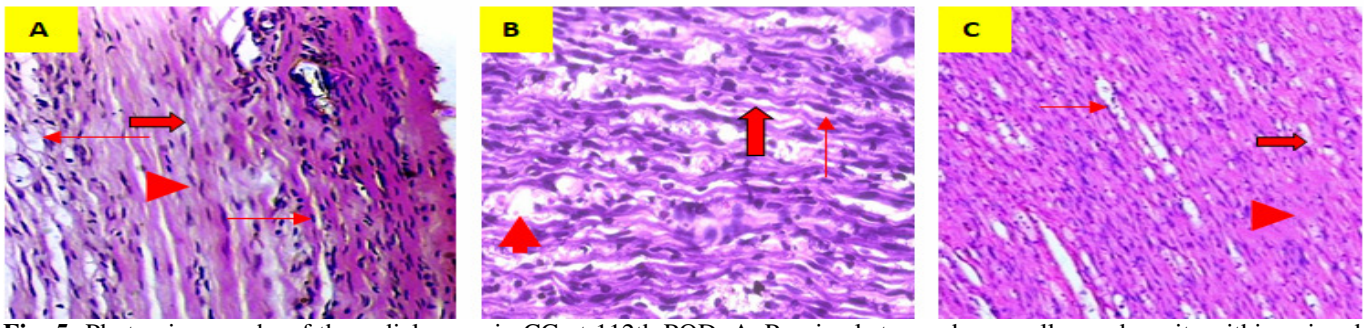

Fig. 5: Photomicrographs of the radial nerve in CG at 112th POD. A. Proximal stump shows collagen deposits within epi and perineurium (thin arrow), regenerated nerve fibers (thick arrow) with Schwann cells (arrowhead), B. Mid site demonstrated the presence of Schwann cells (thin arrow), an improved parallel of nerve fibers (thick arrow), and few depositions of collagen (scar tissue) (arrowhead); C. Distal stump shows some degenerated, vacuolated nerve fibers (thin arrow), minimum scar tissue (thick arrow) with increased of myelinated nerve fibers (arrow head). X40 H&E.

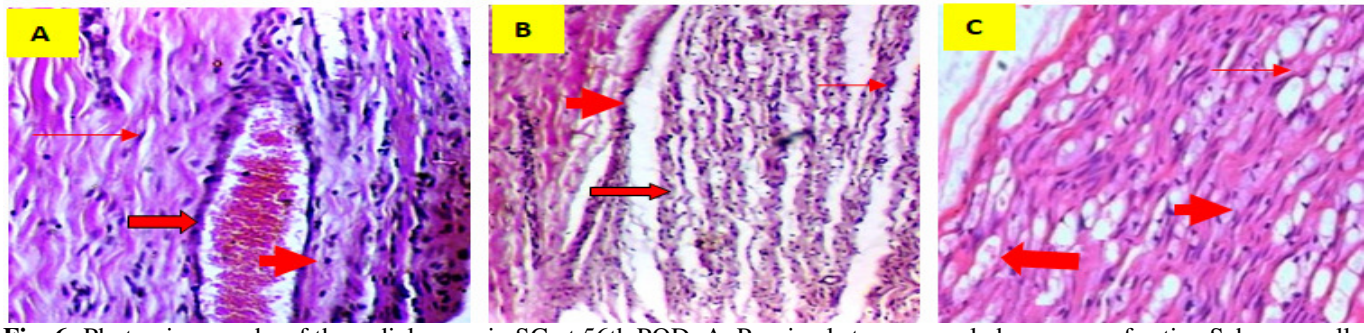

Fig. 6: Photomicrographs of the radial nerve in SG at 56th POD. A. Proximal stump revealed presence of active Schwann cells (thin arrow), angiogenesis (thick arrow), with infiltration of inflammatory cells (arrow head): B. Mid site shows parallel arrangement of new nerve fibers at the site of defect (thick arrow), with basophilic schwann cells (thin arrow), and new angiogenesis (arrow head). C. Distal stump demonstrates degeneration, ovoid (thin arrow), digestive champers (thick arrow), with good orientation of nerve fibers. X40 H&E

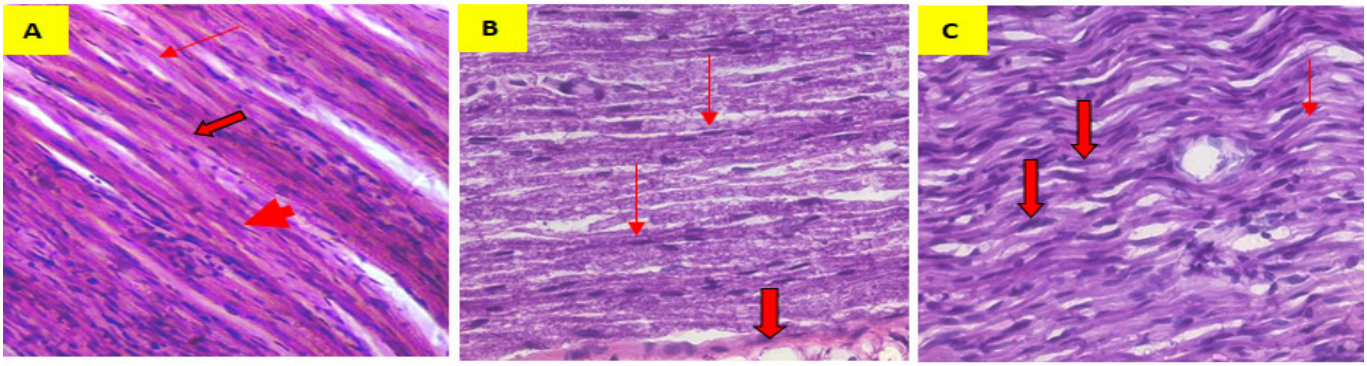

Fig. 7: Photomicrographs of the radial nerve in SG at 112th POD. A. Proximal stump shows improved orientation of the nerve fibers (thin arrow), with good remyelination of the nerve fibers (thick arrow), and presence of active proliferative Schwann cells (arrowhead); B. Mid stump revealed the presence of active Schwann cells (thin arrow), angiogenesis (thick arrow); C. Distal stump shows the parallel orientation of nerve fibers (thin arrow), with plenty numbers of active Schwann cells (thick arrow). X40 H&E.

Discussion

This study demonstrated an improvement in the microscopical sections of the treated animals with the acellular bovine urinary bladder matrix conduit enriched with intraluminal scaffolds of the acellular human umbilical cord as compared with these treated with hallow conduit. This improvement might be due to the effectiveness of the acellularhuman umbilical cord ECM scaffold to elicit many coordinated cellular responses including cell migration, proliferation, and differentiation, modulation of inflammatory responses and activation, and recruitment of stem and progenitors cells leading to the formation of new site-appropriate tissue. These findings are congruent with that of Gardiner, (2011), who reported that the importance of ECM proteins is already visible at the developmental stage of the nervous system, during which fibronectin is mainly involved in the migration and differentiation of the neural crest cells. In contrast, laminin is the main protein involved in the maturation stage of the peripheral nervous system and appears to be crucial for the SC to successfully myelinate axons. Xie and Auld (2011) further demonstrated that integrin complexes play an important role in maintaining the ensheathing layer of glial cells around the axons, dictating and modulating the process of myelination. Also, microscopical sections revealed that there is mild intraneural scaring in the (SG), while remarkable and severe collagen deposits in the sections of (CG). The success of axon regeneration can be viewed as a balance between regeneration and scar formation, and relationship was found between scar tissue formation and axonal regeneration (Kaplan *et al*., 2011). Du *et al.* (2017) used a chitosan nerve guide which was filled with fibrin nanofiber hydrogel, to bridge 10 mm rat sciatic nerve defects comparing it to hollow chitosan tubes, the results revealed better sciatic nerve recovery when compared to the hollow conduit group. Furthermore, the bioengineered grafts supported successful axonal regrowth towards the distal target already 6 weeks after surgery as well as a higher nerve fiber density and remyelination in the distal stump 12 weeks after surgery when compared to empty conduit group. Subsequently, the histopathological sections of the scaffold group (SG) at 56th POD showed presence of numerous active schwann cells and marked angiogenesis, as showed as decreased in their numbers of the conduit group (CG) at 56th POD, and this result suggests that the ECM derived from human umbilical cord has a bioactive and potential therapeutic effects and might participate in the defected radial nerve regeneration. In fact, as reviewed by Daly *et al.,* (2012), the formation of a fibrin-rich scaffold can be usually observed between the proximal and distal stumps in order to guide the following cell migration through an ECM bridge. The natural scaffold forms within 1 week after injury, guiding the migration of SC together with endothelial cells and fibroblasts, to form the bands of Büngner. By using ECM proteins is therefore possible to simulate and engineer the regenerative process as it would naturally occur in vivo. Other studies reported that the fibrous proteins embedded in the ECM include; collagens (90%), fibronectins, laminin and elastin (Schaefer and

Schaefer, 2010). Moreover the sGAG present in ECM includes chondroitin sulfates, heparin, heparan sulfate, and hyaluronic acid, and these structures can bindvarious types of cytokines and growth factors, such as transforming growth factor-β (TGF-β), basic fibroblast growth factor (b-FGF), platelet-derived growth factor (PDGF) and vascular endothelial growth factor (VEGF)and contribute to neural tissue reconstruction (Crapo *et al.,* 2012). On the other hand, the molecular and cellular mechanisms regulating neovascularization and axon regrowth after PN injury are poorly understood. However, recent studies suggest angiogenesis and neurogenesis are closely linked66 and likely modulated by the innate immune response to PN injury (Mokarram *et al.,* 2012). Macrophages are hypothesized to respond to and direct endothelial cell migration and the formation of new blood vessels in hypoxic tissues. In turn, newly formed blood vessels have been shown to guide Schwann cells and hence axon regrowth across PN injuries (Cattin *et al.,* 2015). alternatively activated, anti-inflammatory (M2-like) macrophages are linked to improved PN remodeling and positive outcomes (Enam *et al.,* 2017) and anti-inflammatory signaling can increase Schwann cell differentiation and migration (Clements *et al.,* 2017) and axon growth (Mokarram *et al*., 2012). Moreover, ECM bioscaffolds can increase M2-like macrophage polarization and Schwann cell migration (Prest *et al.,* 2017). After implantation, ECM bioscaffolds are rapidly invaded by macrophages, among other immune cells. Infiltrating macrophages degrade ECM bioscaffolds proteolytically (Valentin *et al.,* 2009), releasing various bioactive matricryptic peptide fragments that can positively modulate the healing response by decreasing inflammatory signaling (Swinehart and Badylak, 2016), and increasing both angiogenesis (D'Amore*et al.,* 2016) and neurogenesis (Agrawal *et al.,* 2009). Whether ECM or macrophage derived factors or macrophages or a combination of the two enter epineurial repair sites to modulate inflammation and tissue repair is unknown. However, recent studies have shown that ECM can release bioactive factors directly into wrapped nerves that can positively modulate both peripheral and central nerve regeneration (Suzuki *et al.,* 2017). Moreover, M2-like macrophages release several anti-inflammatory cytokines and other factors like extracellular vesicles(EVs) (Van der Merwe *et al*., 2017) that can presumably diffuse into the defect site to positively modulate the phenotypes of both resident and other infiltrating immune cells (Van der Merwe *et al.,* 2016).

Conclusion

Histopathological analysis of this experimental study suggests that the acellular and lyophilized human umbilical cord ECM scaffold guided by acellular bovine urinary bladder matrix conduit might be capable of promoting the regeneration of nerve after neurotmesis of the radial nerve.

Acknowledgments

This study was supported by the Coordination College of Veterinary Medicine, University of Baghdad, Iraq.

References

Agrawal, V.; Brown, B.N.; Beattie, A.J.; Gilbert, T.W. and Badylak, S.F. (2016). Evidence of innervation following extracellular matrix scaffold-mediated remodelling of muscular tissues. J. Tissue Eng. Regen. Med., 3: 590–600.

Badylak, S.F.; Dziki, L.J. ; Sicari, B.M. ; Ambrosio, F. and Boninger, M.L. (2016). Mechanisms by which acellular biologic scaffolds promote functional skeletal muscle restoration. Biomaterials., 103: 128–136.

Badylak, S.F.; Freytes, D.O. and Gilbert, T.W. (2009). Extracellular matrix as a biological scaffold material: Structure and function. ActaBiomater., 5: 1–13.

Brown, B.N.; Chung, W.L. ; Pavlick, M.; Reppas, R.; Ochs, M.W.; Russell, A.J. and Badylak, S.F. (2011). Extracellular matrix as an inductive template for temporomandibular joint meniscus reconstruction: a pilot study. J. Oral Maxillofac. Surg., 69: 488–505.

Cattin, A.L.; Burden, J.J.; Emmenis, L.V.; Mackenzie, F.E.; Hoving, J.J.; Calavia, N.G.; Guo, Y.; McLaughlin, M.; Rosenberg, L.H.; Quereda, V.; Jamecna, D.; Napoli, I.; Parrinello, S.; Enver, T.; Ruhrberg, C. and Lloyd, A.C. (2015). Macrophage-Induced Blood Vessels Guide Schwann Cell-Mediated Regeneration of Peripheral Nerves. Cell, 162: 1127–1139.

Cattin, A.L.; Burden, J.J. ; Emmenis, L.V. ; Mackenzie, F.E. ; Hoving, J.J.A.; Calavia, N.G.; Guo, Y.; McLaughlin, M.; Rosenberg, L.H.; Quereda, V.; Jamecna, D.; Napoli, I.; Parrinello, S.; Enver, T.; Ruhrberg, C. and Lloyd, A.C. (2015). Macrophage-Induced Blood Vessels Guide Schwann Cell-Mediated Regeneration of Peripheral Nerves. Cell, 162: 1127–39.

Chen, D.; Chen, S.; Wang, W.; Zhang, C. and Zheng, H. (2011). Spontaneous regeneration of recurrent laryngeal nerve following long-term vocal fold paralysis in humans: Histologic evidence. Laryngoscope, 121:1035–1039.

Chen, J. and Shen, H. (2017). Tissue-engineered nerve conduits with internal structure in the repair of peripheral nerve defects. Zhongguo Zuzhi Gongcheng Yanjiu., 21:1273–1279.

Clements, M.P.; Byrne, E.; Guerrero, L.F.; Cattin, A.L.; Zakka, L. ; Ashraf, A.; Burden, J. J.; Khadayate, S.; Lloyd, A.C.; Marguerat, S. and Parrinello, S. (2017). The Wound Microenvironment Reprograms Schwann Cells to Invasive Mesenchymal-like Cells to Drive Peripheral Nerve Regeneration. Neuron, 96: 98–114.

Crapo, P.M.; Medberry, C.J.; Reing, J.E.; Tottey, S.; van der Merwe, Y.; Jones, K.E. and Badylak, S.F. (2012). Biologic scaffolds composed of central nervous system extracellular matrix. Biomaterials, 33: 3539–5347.

D'Amore, A.; Yoshizumi, T.; Luketich, S.K.; Wolf, M.T.; Gu, X.; Cammarata, M.; Hoff, R.; Badylak, S. and Wagner, W. (2016). Bi-layered polyurethane-Extracellular matrix cardiac patch improves ischemic ventricular wall remodeling in a rat model. Biomaterials, 107: 1–14.

Daly, W.; Yao, L.; Zeugolis, D.; Windebank, A. and Pandit, A. (2012). A biomaterials approach to peripheral nerve regeneration: bridging the peripheral nerve gap and enhancing functional recovery. Interface, 9: 202–221.

di Summa, P.G.; Kalbermatten, D.F.; Pralong, E.; Raffoul, W.P.; Kingham, J. and Terenghi, G. (2011). Long-term in vivo regeneration of peripheral nerves through bioengineered nerve grafts. Neuroscience, 181: 278–291.

Du, J.; Liu, J.; Yao, S.; Mao, H.; Peng, J.; Sun, X.; Cao, Z.; Yang, Y.; Xiao, B.; Wang, Y.; Tang, P. and Wang, X. (2017). Prompt peripheral nerve regeneration induced by a hierarchically aligned fibrin nanofiber hydrogel. ActaBiomater., 55 296–309.

Dziki, J.L.; Huleihel, L.; Scarritt, M.; Badylak, S.F. (2017). Extracellular Matrix Bioscaffolds as Immunomodulatory Biomaterials. Tissue Eng. Part A, 23(19-20):1152-1159.

Eberli, D.; Atala, A. and Yoo, J.J. (2011). One and four layer acellular bladder matrix for facial tissue reconstruction. J. Mater. Sci. Mater. Med., 22:741-751.

Enam, S.F.; Krieger, J.R.; Saxena, T.; Watts, B.E.; Olingy, C.E.; Botchwey, E.A. and Bellamkonda, R.V. (2017). Enrichment of endogenous fractalkine and anti-inflammatory cells via aptamer-functionalized hydrogels. Biomaterials, 142: 52–61.

Faroni, A.; Kingham, P.J. and Reid, A.J. (2015). Peripheral nerve regeneration: experimental strategies and future perspectives. Adv. Drug Deliv. Rev., 83:160–167.

Faust, A; Kandakatla, A.; Merwe, Y.; Ren, T.; Huleihel, L. and Steketee, M. (2017). Urinary bladder extracellular matrix hydrogels and matrix-bound vesicles differentially regulate central nervous system neuron viability and axon growth and branching. J. Biomater. Appl., 31: 1277–1295.

Fercana, G.R.; Yerneni, S.; Billaud, M.; Hill, J.; VanRyzin, P.; Richards, T.; Sicari, B.; Johnson, S.; Badylak, S.; Campbell, P.; Gleason, T. and Phillippi, J. (2017). Perivascular extracellular matrix hydrogels mimic native matrix microarchitecture and promote angiogenesis via basic fibroblast growth factor. Biomaterials, 123: 142–154.

Gardiner, N.J. (2011). Integrins and the extracellular matrix: key mediators of development and regeneration of the sensory nervous system. Dev. Neurobiol., 71: 1054–1072.

Gonzalez-Perez, F.; Cobianchi, S.; Heimann, C.; Phillips, J.B.; Udina, E. and Navarro, X. (2017). Stabilization, rolling, and addition of other extracellular matrix proteins to collagen hydrogels improve regeneration in chitosan guides for long peripheral nerve gaps in rats. Neurosurgery., 80: 465–474.

Gonzalez-Perez, F.; Udina, E. and Navarro, X. (2013). Extracellular matrix components in peripheral nerve regeneration. Int. Rev. Neurobiol., 108:257–275.

Hoben, G.; Yan, Y.; Iyer, N.; Newton, P.; Hunter, D.A.; Moore, A.M.; Sakiyama-Elbert, S.A.; Wood, M.D. and Mackinnon, S.E. (2015). Comparison of acellular nerve allograft modification with Schwann cells or VEGF. Hand (N Y), 10: 396–402.

Hoke, A. and Brushart, T. (2010). Introduction to special issue: Challenges and opportunities for regeneration in the peripheral nervous system. Exp. Neurol., 223: 1–4.

Hong, Y.; Huber, A.; Takanari, K.; Amoroso, N.; Hashizume, R.; Badylak, S. and Wagner, W. (2011). Mechanical properties and in vivo behavior of a biodegradable synthetic polymer microfiber-extracellular matrix hydrogel biohybrid scaffold. Biomaterials, 32: 3387–3394.

Houshyar, S.; Bhattacharyya, A. and Shanks, R. (2019). Peripheral nerve conduit: materials and structures. ACS Chem. Neurosci., 10: 3349–3365.

Jesuraj, N.J.; Santosa, K.B.; Macewan, M.R.; Moore, A.M.; Kasukurthi, R. and Sakiyama-Elbert, S.E. (2014). Schwann cells seeded in acellular nerve grafts improve functional recovery. Muscle Nerve, 49: 267–276.

Kanno, H.; Pearse, D.D.; Ozawa, H.; Itoi, E. and Bunge, M.B. (2015). Schwann cell transplantation for spinal cord injury repair: Its significant therapeutic potential and prospectus. Rev. Neurosci., 26: 121–128.

Kaplan, S.; Piskin, A.; Ayyildiz, M.; Aktaş, A.; Köksal, B.; Ulkay, M.; Türkmen, A.; Bakan, F. and Geuna, S. (2011). The effect of melatonin and platelet gel on sciatic nerve repair: an electrophysiological and stereological study. Microsurgery, 31(4): 306–313.

Khuong, H.T; Kumar, R.; Senjaya, F.; Grochmal, J. and Midha, R. (2014). Skin derived precursor Schwann cells improves behavioral recovery for acute and delayed nerve repair. Exp. Neurol., 254: 168–79.

Lavasani, M.; Thompson, S.D.; Pollett, J.B.; Usas, A.; Lu, A.; Stolz, D.B.; Clark, K.A.; Sun, B.; Péault, B. and Huard, J. (2014). Human muscle-derived stem/progenitor cells promote functional murine peripheral nerve regeneration. J. Clin. Invest., 124: 1745–56.

Li, J.; Hansen, K.C.; Zhang, Y.; Dong, C.; Dinu, C.Z.; Dzieciatkowska, M. and Pei, M. (2014). Rejuvenation of chondrogenic potential in a young stem cell microenvironment. Biomaterials, 35: 642–653.

Liu, T.D.; Zhang, B.C. and Hao, M.L. (2017). Collagen-gelatin scaffolds for the repair of peripheral nerve defects. Zhongguo Zuzhi Gongcheng Yanjiu., 21: 286–290.

Luna, L.G. (1992). Histopathologic methods and color atlas of special stains and tissue artifacts. Maryland: American Histolabs, Inc.

Meng, F.; Modo, M.; and Badylak, S.F. (2014). Biologic scaffold for CNS repair. Regen. Med., 9: 367–383.

Mokarram, N.; Merchant, A.; Mukhatyar, V.; Patel, G. and Bellamkonda, R.V. (2012). Effect of modulating macrophage phenotype on peripheral nerve repair. Biomaterials, 33: 8793–8801.

Prest, T.A.; Yeager, E.; LoPresti, S.T.; Zygelyte, E.; Martin, M.J.; Dong, L.; Gibson, A.; Olutoye, O.; Brown, B.N. and Cheetham, J. (2017). Nerve-specific, xenogeneic extracellular matrix hydrogel promotes recovery following peripheral nerve injury. J. Biomed. Mater. Res. A, 106:450–459.

Remlinger, N.T.; Gilbert, T.W. and Wearden, P.D. (2013). Urinary bladder matrix promotes site appropriate tissue formation following right ventricle outflow tract repair. Organogenesis, 9: 149–160.

Rosario, D.J.; Reilly, G.C.; Salah, E.A.; Glover, M.; Bullock, A.J. and Macneil, S. (2008). Decellularization and sterilization of porcine urinary bladder matrix for tissue engineering in the lower urinary tract. Regen. Med., 3(2): 145-156.

Sabongi, R.G.; Fernandes, M. and J. Dos Santos, (2015). Peripheral nerve regeneration with conduits: Use of vein tubes. Neural Regen. Res., 10: 529–533.

Schaefer, L. and Schaefer, R.M. (2010). Proteoglycans: from structural compounds to signaling molecules. Cell Tissue Res., 339: 237-246.

Siemers, F. and Houschyar, K.S. (2017). Alternative Strategies for Nerve Reconstruction. Modern Concepts

of Peripheral Nerve Repair. 1. Cham, Switzerland: Springer, pp. 127–138.

Suzuki, K.; Tanaka, H.; Ebara, M.; Uto, K.; Matsuoka, H.; Nishimoto, S.; Okada, K.; Murase, T. and Yoshikawa, H. (2017). Electrospunnanofiber sheets incorporating methylcobalamin promote nerve regeneration and functional recovery in a rat sciatic nerve crush injury model. ActaBiomate., 53: 250–259.

Swinehart, I.T. and Badylak, S.F. (2016). Extracellular matrix bioscaffolds in tissue remodeling and morphogenesis. Dev. Dyn., 245(3): 351-360.

Valentin, J.E.; Stewart-Akers, A.M.; Gilbert, T.W. and Badylak, S.F. (2009). Macrophage participation in the degradation and remodeling of extracellular matrix scaffolds. Tissue Eng. Part A 15: 1687–1694.

Van der Merwe, Y. and Steketee, M.B. (2016). Immunomodulatory approaches to CNS injury: extracellular matrix and exosomes from extracellular matrix conditioned macrophages. Neural Regen. Res., 11: 554–556

Van der Merwe, Y.; Faust, A.E. and Steketee, M.B. (2017). Matrix bound vesicles and miRNA cargoes are bioactive factors within extracellular matrix bioscaffolds. Neural Regen. Res., 12: 1597–1599.

Xie, X. and Auld, V.J. (2011). Integrins are necessary for the development and maintenance of the glial layers in the Drosophila peripheral nerve. Development, 138: 3813–3822.

Yao, Y.; Cui, Y.; Zhao, Y.; Xiao, Z.; Li, X.; Han, S.; Chen, B.; Fang, Y.; Wang, P.; Pan, J. and Dai, J. (2018). Effect of longitudinally oriented collagen conduit combined with nerve growth factor on nerve regeneration after dog sciatic nerve injury. J. Biomed. Mater. Res. B Appl. Biomater., 106: 2131–2139.